


# CO<sub>2</sub> absorption intensification using three-dimensional printed dynamic polarity packing in a bench-scale integrated CO<sub>2</sub> capture system

Min Xiao<sup>1</sup>  | Moushumi Sarma<sup>1</sup> | Jesse Thompson<sup>1,2</sup> | Du Nguyen<sup>3</sup> | Samantha Ruelas<sup>3</sup> | Kunlei Liu<sup>1,4</sup>

<sup>1</sup>Center for Applied Energy Research,  
University of Kentucky, Lexington,  
Kentucky, USA

<sup>2</sup>Department of Chemistry, University of  
Kentucky, Lexington, Kentucky, USA

<sup>3</sup>Lawrence Livermore National Laboratory,  
Livermore, California, USA

<sup>4</sup>Department of Mechanical Engineering,  
University of Kentucky, Lexington,  
Kentucky, USA

## Correspondence

Jesse Thompson and Kunlei Liu, University of  
Kentucky, 2540 Research Park Drive,  
Lexington, KY, USA.  
Email: jesse.thompson@uky.edu and  
kunlei.liu@uky.edu

## Funding information

U.S. Department of Energy, Grant/Award  
Number: DE-FE0031661

## Abstract

Postcombustion carbon capture using a chemical absorbent is a promising technology to reduce CO<sub>2</sub> emission. However, the overall construction and operating costs remain a major challenge. In order to intensify the absorption process and to reduce these costs, a novel dynamic polarity structured packing (DP packing) with alternate patterns of surface polarity has been developed to enhance local macro-scale turbulence within the advanced viscous solvent to reduce the mass transfer diffusion resistance. Three DP structured packings that incorporate multiple polymeric materials were fabricated using three-dimensional printing technique and evaluated through parametric testing using a bench-scale integrated CO<sub>2</sub> capture unit with 76.2 mm ID absorber. At optimized operating conditions, the DP packing showed a relative 22.7% increase in absorption and 20.0% decrease in energy penalty.

## KEYWORDS

aqueous amine, CO<sub>2</sub> capture, dynamic polarity packing, mass transfer intensification

## 1 | INTRODUCTION

Reducing CO<sub>2</sub> emission from the burning of fossil fuel plays key role in the context of carbon neutrality. Several strategies have been proposed in this regard which can be commonly categorized into liquid-based CO<sub>2</sub> absorption and solid-based CO<sub>2</sub> adsorption.<sup>1</sup> Among those strategies, postcombustion capture of CO<sub>2</sub> (PCC) using liquid absorbents is suitable for dilute, low-pressure flue gas streams from fossil fuel-based power stations.<sup>2</sup> It can be readily retrofitted to the existing power plants and has emerged as a very promising technology for gas separation. However, the commercialization of large-scale PCC is still limited due to the high construction and operating costs and the lack of national energy policy. Improving the mass transfer and decreasing the energy penalty is critical to reduce the total cost of CO<sub>2</sub> capture and boost the technology deployment. One possible way is to intensify mass transfer during CO<sub>2</sub> absorption.

For the liquid-based CO<sub>2</sub> capture, the absorption happens in an absorber column filled with packings to provide a large interfacial area

forming a thin liquid film for the efficient mass transfer<sup>3</sup> due to the nature of its slow reaction kinetics. Structured packings are widely used to handle the large gas volume with low resistance.<sup>4,5</sup> They can guide the solvent through a designated path for low-pressure drop and less liquid holdup. Many works have demonstrated that structured packings could provide a large effective interfacial surface to realize efficient CO<sub>2</sub> removal from combustion flue gas.<sup>6–8</sup> Although the dimension of the absorber column is significantly reduced as a result of the existing structured packings, it is still one of the largest and priciest device in the purchased equipment for absorption-based CO<sub>2</sub> capture plant.<sup>9</sup>

In addition, many advanced absorbents have been proposed for low regeneration energy cost but meanwhile they are facing the rise of viscosity.<sup>10,11</sup> As well known, increasing absorbent viscosity leads to lower diffusivity within the liquid phase,<sup>12</sup> larger liquid holdup,<sup>13,14</sup> and thicker liquid film,<sup>15,16</sup> which means greater mass transfer resistance for CO<sub>2</sub> absorption.<sup>17</sup> Some researchers studied the mass transfer intensification for gas absorption in viscous absorbent through

stronger turbulence and better mixing effect within the liquid phase.<sup>18–20</sup> However, these works were carried out in the existing plate surface and the turbulence was realized through the mechanical modifications, which might decrease the surface area and increase the liquid holdup.

In this work, we propose novel structured packings namely dynamic polarity packing (DP packing) to apply the polarity difference of fabrication materials to drive macro-scale turbulence hydraulically through a selected pattern. The *in situ* manipulation of flow hydraulic through alternating the surface with relative hydrophilicity and hydrophobicity enables DP packing to entirely mimic the geometry of conventional packings without additional mechanical obstacles. Three different DP packings were successfully fabricated via three-dimensional (3D) printing using nylon and high-impact polystyrene (HIPS or known as high-density polystyrene [HDPS]) as coprinting polymers. These packings were tested in a bench-scale integrated CO<sub>2</sub> capture unit and compared with Mellapak 250 Y steel packings in terms of CO<sub>2</sub> absorption and energy consumption. CAER Amine-based Solvent developed by UK CAER was used in test.<sup>21</sup> A new parameter namely normalized free amine was proposed to evaluate

packings performance on mass transfer. The contact angle of the amine solvent on steel, nylon, and HIPS surface was measured to quantify their wettability. The operating conditions were optimized for the current integrated CO<sub>2</sub> capture unit and the role of the DP packings in PCC was revealed.

## 2 | EXPERIMENTAL METHODS

### 2.1 | Materials

CO<sub>2</sub> (99.9%) and span gas (14 vol% CO<sub>2</sub> gas) were purchased from Scott-Gross Company, Inc. Phosphoric acid (≥85 wt%, Sigma-Aldrich) was used as received.

### 2.2 | Integrated bench-scale unit

CO<sub>2</sub> capture experiments were carried out in an integrated CO<sub>2</sub> capture bench-scale unit as shown in Figure 1. The system mainly includes

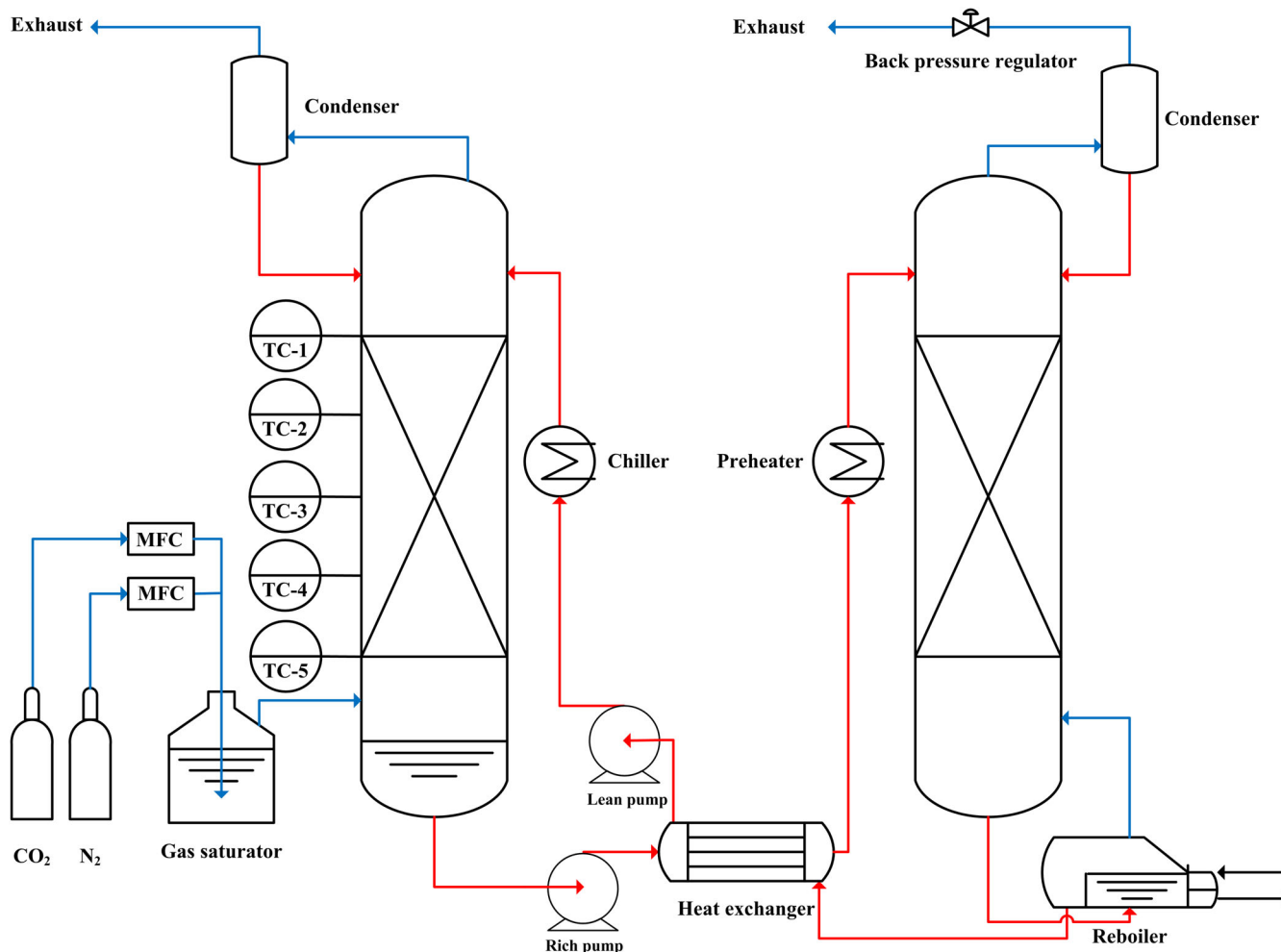


**FIGURE 1** Simplified schematic of integrated CO<sub>2</sub> capture bench-scale unit where blue line refers to vapor line and red line indicates liquid line

three fluid circulations namely absorbent, hot oil (for stripper energy supply), and cooling water for mass and/or heat transfer to realize continuous CO<sub>2</sub> removal from the mixture gas of CO<sub>2</sub> and N<sub>2</sub>. The gas flow rate is controlled by GFC mass flow controllers (Aalborg Instruments & Controls Inc.) to adjust CO<sub>2</sub> concentration. The gas is then sent to the bottom of a 76.2-mm ID transparent PVC absorber column for absorption. A saturator is set to moisturize the gas for solvent quality management. The CO<sub>2</sub> content is monitored using Horiba VIA-510 CO<sub>2</sub> analyzers (Horiba, Ltd.). CO<sub>2</sub> lean solvent is pumped to the top of the absorber column for countercurrent flow with upward gas. After absorption, CO<sub>2</sub>-rich solvent is pumped to the stripper for regeneration and the regenerated solvent will be sent back to the absorber for cyclic absorption. The stripper has a 76.2-mm ID stainless steel column filled with 6 × 6-mm ceramic raschig rings. A hot oil-jacketed reboiler is applied at the bottom of the stripper as the heat source. There are condensers at top of both the absorber and the stripper column for water balance and emission control. A heat exchanger is employed to recover the heat of lean solvent stream existing reboiler and raise rich solvent temperature. A chiller is used to tune lean solvent inlet temperature and an additional preheater is set to further increase the rich solvent temperature before it enters the stripper. At each condition, the unit is operated under steady state for at least 2 h during which all the operation parameters remain barely changed. LabVIEW 2010 is used to control the system and collect data.

## 2.3 | Solvent analysis and properties

Liquid samples were taken from rich and lean streams after the system reached a steady state. The alkalinities of the samples were obtained using an auto titrator (Metrohm 888 Titrando). CO<sub>2</sub> loading measurements were carried out through inorganic carbon analysis by phosphoric acid treatment as shown in Figure S1. A quantitative amount of sample was injected into the column containing excessive phosphoric acid. The N<sub>2</sub> gas was used as carrier gas to continuously deliver the released CO<sub>2</sub> to a calibrated CO<sub>2</sub> analyzer. The signals were collected and integrated into a computer to obtain CO<sub>2</sub> loading. The data reliability was verified using standard potassium carbonate samples.

The contact angles were acquired at 22°C on a Biolin Scientific Optical Tensiometer, using Oneattention software. The contact angle was measured on a polished surface of stainless steel, nylon, and HIPS by the sessile drop method. All the measurements were recorded in triplicates and the average value of all three measurements was reported. The CAER Solvent under different conditions (with or without additive, CO<sub>2</sub> loading at 0, 0.247, and 0.471 mol CO<sub>2</sub>/mol amine) were used in the contact angle measurement.

In terms of the solvent properties: The lean CO<sub>2</sub> loading covers wider range from 0.119 to 0.364 mol CO<sub>2</sub>/mol amine while rich CO<sub>2</sub> loading shows a range from 0.350 to 0.472 mol CO<sub>2</sub>/mol amine. For the lean solvent, the viscosity is around 4 mPa s at 40°C, the density is about 105 kg m<sup>-3</sup> at 25°C and the surface tension is close to 50 mN/m at 22°C. Increasing CO<sub>2</sub> loading slightly changes the physical properties.

## 2.4 | Structured packing

The baseline 3D-printed packing geometry files were generated using Blender to mimic the geometric structure of Mellapak 250Y. The internal packing structure was generated from an initial corrugated surface with a crest-to-crest pitch of 25.4 mm and a depth of 12.7 mm. The texture was added to the structure by introducing a secondary XY corrugation with a pitch of 4 mm and a height of 0.5 mm. A square grid of perforations was designed into the structure with a 4.5-mm hole diameter and spacing of 12.7 mm between each perforation. The corrugated packing elements were stacked at an angle of 45° relative to the z axis and each layer was set perpendicular to the previous element. The combined corrugated packing elements were constrained to a cylindrical volume with a diameter of 73 mm and a height of 152.4 mm. A secondary shell geometry with an outer diameter of 75 mm and a shell thickness of 1 mm was added to enclose the packed structure for strength enhancement. More detailed information of packing fabrication can be found in Appendix S1.

## 3 | CALCULATIONS

The CO<sub>2</sub> absorption rate is calculated based on the inlet and outlet CO<sub>2</sub> mole flow rate in simulate gas and exhaust gas. The CO<sub>2</sub> absorption efficiency is calculated using Equation (1).

$$\phi_{\text{CO}_2} = \frac{n_{\text{CO}_2}^{\text{in}} - n_{\text{CO}_2}^{\text{out}}}{n_{\text{CO}_2}^{\text{in}}} \times 100\% \quad (1)$$

where  $n_{\text{CO}_2}^{\text{in}}$  is inlet CO<sub>2</sub> mole flow rate, mol/s;  $n_{\text{CO}_2}^{\text{out}}$  is outlet CO<sub>2</sub> mole flow rate, mol/s.

The preheater heat duty and reboiler duty is calculated by Equation (2) because the temperature difference between inlet and outlet of heating fluid of reboiler is very small, less than 7 °C:

$$Q = C_p^{\text{fluid}} m_{\text{fluid}} \rho_{\text{fluid}} (T_R^{\text{in}} - T_R^{\text{out}}) \quad (2)$$

where  $C_p^{\text{fluid}}$ ,  $m_{\text{fluid}}$ , and  $\rho_{\text{fluid}}$  is heat capacity (kJ/g/K), flow rate (L/s), and density (g/L) of fluid;  $T_R^{\text{in}}$  is inlet temperature, K;  $T_R^{\text{out}}$  is outlet temperature, K.

The energy demand (E, kJ/mol CO<sub>2</sub>) is calculated through Equation (3):

$$E = Q / (n_{\text{CO}_2}^{\text{in}} - n_{\text{CO}_2}^{\text{out}}) \quad (3)$$

## 4 | RESULTS AND DISCUSSION

For the CO<sub>2</sub> capture experiments in the integrated unit, solvent alkalinity was maintained around 5 mol/kg in the practical operation. The

system operation parameters are summarized in Table 1 where most of the operation parameters are fixed during the operation. Three parameters, namely solvent circulation rate, stripper pressure, and heat duty, are varied to study their influences on the system while the total gas flow rate being maintained constant. The solvent circulation rate has three levels from 300 to 600 ml/min to yield L/G ratios at 1.7, 2.6, and 3.5 kg/kg. The stripper top pressure is adjusted between 120 and 180 kPa. The heat duty to reboiler ranges from 1.4 to 3.0 kW depending on the hot oil temperature. The combination of these conditions requires the solvent regeneration temperature ranges from 105 to 120°C. It is worth mentioning that the lean-rich heat exchanger is not optimized in this small bench-scale unit where the approach temperature is much larger than the conventional 10°C adopted for most PCC. Thus an additional preheater is used to provide supplemental energy to increase the rich solvent temperature at a preferable value before entering the stripper. The system energy input from both preheater and reboiler are considered to calculate final heat duty and energy demand. Consequently, there will be a higher sensible heat, and the energy consumption on CO<sub>2</sub> capture computed from this study will be used only in relative comparison rather than as absolute value. The carbon balance between CO<sub>2</sub> removed from simulated gas and absorbed in solvent is summarized in Figure S2 to show a good agreement in gas and liquid-phase data.

#### 4.1 | Design of dynamic polarity packings

Continuous CO<sub>2</sub> absorption will quickly consume free amine at the interface, leading to less available amine for reaction, which means CO<sub>2</sub> molecule needs to diffuse from liquid surface to bulk liquid for further absorption. This issue is more severe for viscous absorbent which has low diffusivity and thicker liquid film flow on the packings. Accordingly, DP packing is designed to overcome the diffusion limitation. As shown in Figure 2, the relative polar surface tends to draw aqueous solvent and show better wettability (Figure 2A—more hydrophilic) while the relative nonpolar surface with less wettability (Figure 2B—more hydrophobic) will repel the solvent and force it to congregate. Between polar and nonpolar segment, the difference in wettability will enhance local turbulence within the solvent to refresh the liquid surface with assistance of flue gas and expose more free amine molecules from bulk liquid to the liquid surface (Figure 2C) for reaction.

**TABLE 1** Operation parameters in the integrated bench-scale unit

Process variables	Value
Solvent circulation rate (ml/min)	300, 450, 600
Lean solvent return temperature (°C)	40
Gas inlet temperature (°C)	30
Gas CO <sub>2</sub> concentration (vol %)	14%
Gas flow rate (L/min)	127
Stripper top pressure (kPa)	120, 150, 180
Reboiler bulk solvent temperature (°C)	105–120
Heat duty (kW)	1.4–3.0

To quantify the wettability of nylon, HIPS, and steel surfaces, the contact angle was measured using CAER Solvent and the results were summarized in Figure 3. As expected, increasing CO<sub>2</sub> loading will lead to a larger contact angle on all surfaces. This is because the CO<sub>2</sub> loaded solvent shows stronger molecular interactions, lower polarity, and cohesive force to increase the surface tension, forcing the liquid to assemble against solid surface.<sup>22</sup> Comparing different material surfaces, the contact angle of CAER Solvent can be ranked as steel < nylon < HIPS. It means steel surface has the best wettability for CAER Solvent while HIPS surface shows worst wettability. CAER Solvent contains a surfactant-like additive which reduces surface tension from ~60 to 50 mN/m. It is interesting to find that, additive in CAER Solvent only leads to contact angle decrease on nylon and HIPS surface. This brings the contact angle on the steel surface to a similar level as that on the nylon surface. It means there will not be a significant difference in wettability for those two materials if CAER Solvent with additive is used for CO<sub>2</sub> absorption. The contact angle data highlight the benefit of using surfactant-like additive to decrease the solvent surface tension when polymeric packings are used for absorber construction and cost reduction. It also needs to be mentioned that the additive can either increase or decrease mass transfer at gas–liquid interface depending on its concentration.<sup>23–25</sup> In this study the concentration of the additive was selected based on lab-scale screening during which mass transfer was enhanced. For the DP packings containing nylon and HIPS, the contact angle shows around 13–18° difference on those two materials to serve as driving force for enhancing turbulence as highlighted in Figure 2.

Three DP packings noted as DP-1, DP-2, and DP-3 are fabricated as shown in Figure 4 together with Mellapak 250 Y steel packing purchased separately from Koch-Glitch. The DP packings have the same geometric general structure as the steel packing with an additional HIPS shell. The internal packing surface is printed according to the different patterns as shown in the bottom right corner of each figures. DP-1 and DP-3 packings have 5% (of total surface) of HIPS embedded in the nylon packing surface with smooth transition flat plane between two materials, where the HIPS segment is in the form of a staggered rectangle strip for DP-1 and a “V” shape for DP-3. DP-2 packings have alternative full 12.7-mm segments with HIPS (50% of total surface) and nylon (50% of total surface). The solvent from the hydrophilic segment will either pass over a hydrophobic packing surface or be repelled by the hydrophobic shell before entering the next hydrophilic segment, which is expected to sufficiently improve the liquid spread and mixing effect within the absorbent. In the preliminary experiments, it was found that the temperature bulge existed at the upper part of the absorber column under given conditions, indicating that the majority of the CO<sub>2</sub> is captured in this section. Therefore, each type of DP packing was printed in total 457.2 mm and installed in the upper part of the absorber column during the tests.

#### 4.2 | Parametric study and packing evaluation

Although plenty of work toward CO<sub>2</sub> capture system has been carried out in laboratory- and pilot scale, there is the necessity to optimize

**FIGURE 2** Liquid drop of 5 mol/kg CAER Solvent on relative hydrophilic ((A) nylon) and hydrophobic ((B) HIPS) surface. The functional mechanism of DP packing (C)

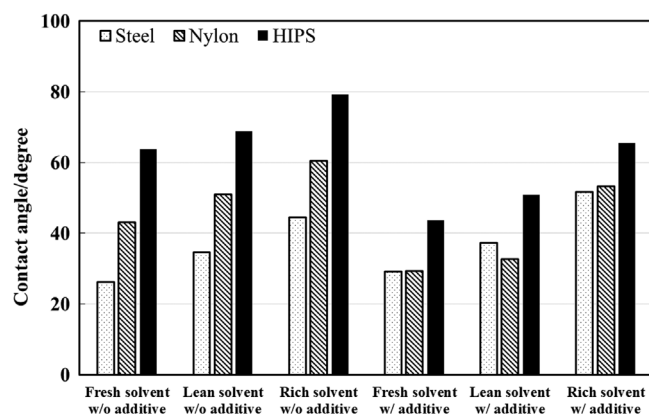
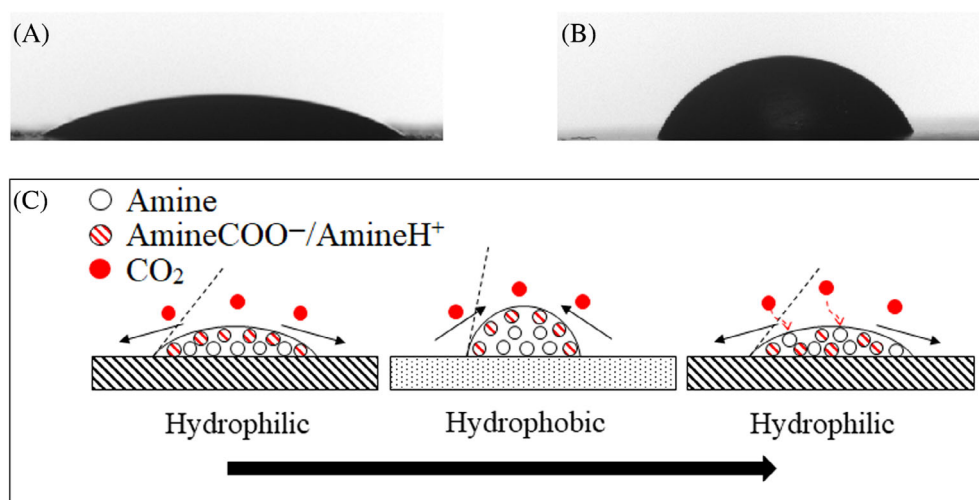


**FIGURE 3** Contact angle of CAER Solvents on different surfaces. The CO<sub>2</sub> loading of fresh, lean, and rich solvent are 0, 0.247, and 0.471 mol CO<sub>2</sub>/mol amine

the operation conditions case by case considering the different CO<sub>2</sub> absorbent and devices.<sup>26</sup> A parametric study was carried out for each packing installed to optimize operating conditions. The CO<sub>2</sub> capture results for all cases were summarized in Figure 5 in terms of absorption efficiency and the energy demand at corresponding run. The bubble size indicates the relative heat duty at corresponding condition.

In general, when comparing with steel packings, the application of DP packings enables the cases to be shifted toward the further bottom right of Figure 5 which means an improved system performance. The cases using DP-3 packing exhibit the best performance of high CO<sub>2</sub> absorption efficiency and low energy demand. The typical conditions of parametric study using DP-1 packing are tabulated in Table 2 to highlight the influence of the L/G ratio and stripper pressure. Changing the L/G ratio could affect liquid holdup in the column while absorbent residence time could vary in the reboiler due to the constant system liquid inventory. Increasing stripper pressure requires high solvent regeneration temperature and impacts the gaseous CO<sub>2</sub>/H<sub>2</sub>O ratio at stripper top. These would cooperatively impact CO<sub>2</sub>

loading in the lean/rich absorbent and working performance of the absorber/stripper. Overall, operating under 2.6 L/G ratio and medium to high stripper pressure is optimal for the current unit regarding both CO<sub>2</sub> absorption efficiency and energy demand. Such influences are similar for those cases using different packings.

In the experiments with fixed packing height, the improvement in mass transfer with DP packings may not be revealed if the packing height is oversized. Thus, a group of cases operated under similar L/G ratio (2.6 kg/kg) and stripper pressure (~120 kPa) are specifically extracted for quantitative comparison, as summarized in Figure 6 in terms of CO<sub>2</sub> absorption efficiency and energy demand. All three DP packings have better performance than steel packing under given conditions. Using Mellapak 250Y steel packing as the baseline, there is a relative 7.8%, 7.7%, and 9.1% improvement in CO<sub>2</sub> absorption efficiency and consequential 7.0%, 7.9%, and 8.4% energy penalty reduction for DP-1, DP-2, and DP-3 packings, respectively. Higher heat duty improves CO<sub>2</sub> absorption efficiency by returning leaner solvent to the absorber which could be interpreted the mass transfer is dominantly controlled by reaction kinetic and the diffusion resistance is minimized with application of DP Packings.

### 4.3 | Mass transfer behavior in the absorber column

The lean CO<sub>2</sub> loading is critical for mass transfer and widely used to correlate CO<sub>2</sub> absorption performance. The CO<sub>2</sub> loading of CAER Solvent that enters (lean) and exits (rich) the absorber column for all cases is summarized in Figure S3 following the order of lean solvent CO<sub>2</sub> loading. Although the rich CO<sub>2</sub> loading is affected by various parameters such as L/G ratio, absorption temperature, packings, and so on, its upper limit is thermodynamically limited by CO<sub>2</sub> gaseous pressure and local temperature.

Nevertheless, the higher lean CO<sub>2</sub> loading does not necessary link to worse CO<sub>2</sub> removal rate when DP packings were used. Increasing the liquid flow rate could counter its effect by providing more free



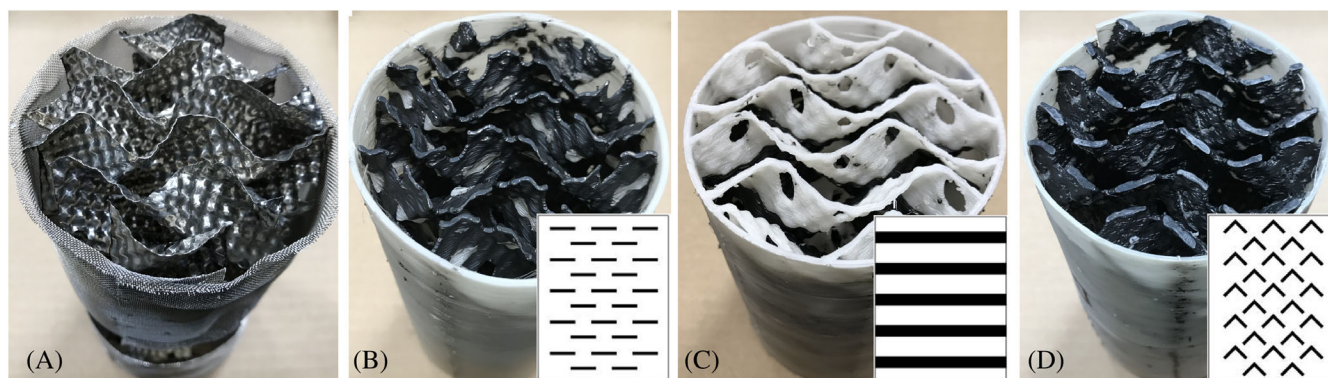


**FIGURE 4** Packings with same geometric structure and different fabrication materials. (A) Mellapak 250Y steel packing; (B) DP-1 packing; (C) DP-2 packing; (D) DP-3 packing

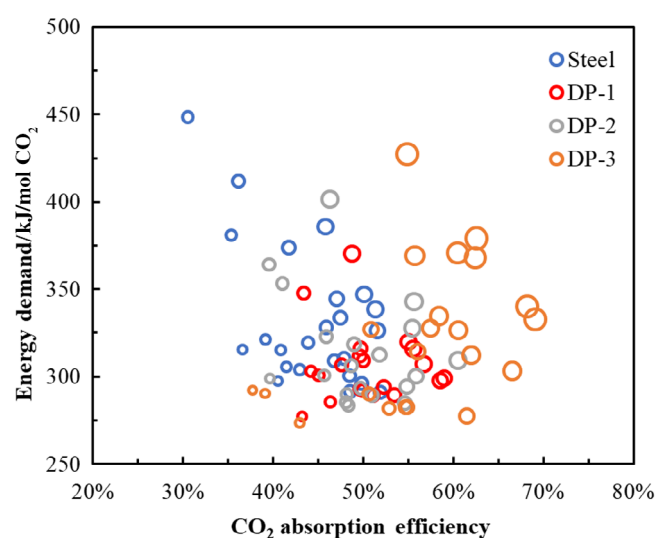


**FIGURE 5** Energy demand versus CO<sub>2</sub> absorption efficiency for all cases through parametric study, where bubble width indicates the heat duty

amine for reaction. For a fair comparison between the cases under different operation conditions, normalized free amine is proposed here to correlate with CO<sub>2</sub> absorption performance in the absorber column. The normalized free amine parameter is defined as the mole of free amine per kilogram gas. Speciation profiles of 5 mol/kg CAER Solvent are presented in Figure S4 to clarify the calculation for normalized free amine. The species concentration is predicted based on the activity coefficient thermodynamic model as described in the previous work.<sup>27</sup> The concentration of free amine decreases with CO<sub>2</sub> absorption to form protonated amine and carbamate products. Before the carbon loading reaching 0.5 mol CO<sub>2</sub>/mol amine, the absorbed CO<sub>2</sub> mainly presents in the form of carbamate and the formation of bicarbonate and carbonate attributes less than 4% to total CO<sub>2</sub> loading. Hence, normalized free amine can be calculated through Equation (4) and influences from L/G, alkalinity, and CO<sub>2</sub> loading on CO<sub>2</sub> absorption are all lumped into one parameter. The benefit of this parameter is that for a certain amount of normalized free amine, the solvent capability to absorb CO<sub>2</sub> is fixed regardless of the L/G ratio or CO<sub>2</sub> loading, or solvent concentration.

**TABLE 2** Parameters of several studied cases using DP-1 steel packings

	L/G (kg/kg)	Q (kW)	Stripper top pressure (kPa)	Reboiler bottom temperature (°C)	Normalized free amine (lean, mol/kg gas)	Lean CO <sub>2</sub> loading(mol CO <sub>2</sub> / mol amine)	Rich CO <sub>2</sub> loading(mol CO <sub>2</sub> / mol amine)	$\phi_{\text{CO}_2}$ (%)	E <sup>a</sup> (kJ/mol CO <sub>2</sub> )
1	1.72	2.27	115	107.1	5.3	0.181	0.403	48.8	370
2	2.60	2.21	118	107.4	6.3	0.251	0.422	55.0	320
3	3.44	2.19	119	107.2	7.3	0.272	0.436	56.7	307
4	1.73	1.97	149	114.2	6.0	0.143	0.409	49.7	316
5	2.57	1.95	150	113.8	6.6	0.235	0.422	53.5	290
6	3.44	1.94	149	111.6	5.4	0.328	0.446	50.0	309
7	1.73	1.85	180	120.4	6.1	0.134	0.430	51.0	289
8	2.60	1.83	181	117.7	5.0	0.297	0.448	47.6	307
9	3.49	1.90	180	114.7	4.3	0.364	0.462	43.4	348

<sup>a</sup>The energy demand includes energy input from both preheater and reboiler.

This helps to eliminate the variance of chemical reaction and reveal the physical mass transfer behavior.

$$\text{Normalized free amine} = (\text{Alk} - 2 \times \text{CL}) \times \frac{L}{G} \quad (4)$$

where Alk is solvent alkalinity and CL is  $\text{CO}_2$  loading, both in terms of mol/kg. It is noted that the unit of normalized free amine is converted to mol/kg gas according to Equation (4).

The relationship between  $\text{CO}_2$  capture rate and normalized free amine in the lean solvent is presented in Figure 7 with different packings. Not surprisingly, a higher concentration of normalized free amine increases  $\text{CO}_2$  capture rate. For steel packing (Figure 7A), it is shown that increasing the L/G ratio decreases the  $\text{CO}_2$  capture rate at same normalized free amine and the decrease is more obvious when the L/G ratio reaches 3.5 kg/kg. As mentioned earlier, the same normalized free amine means equivalent chemical absorption power in the absorbent. However, a higher L/G ratio means larger liquid holdup

and thicker liquid film flow on the steel packing surface, which would hamper the reactant diffusivity. In addition, there needs higher  $\text{CO}_2$  loading in the lean solution to maintain the same normalized free amine at increased L/G ratio. This will lead to a larger contact angle as another downside for mass transfer. Instead, the  $\text{CO}_2$  capture rate at different L/G ratio lies around the same trendline when DP-1 (Figure 7B) packing is used. It means the DP packing can realize comparable mass transfer even at increased L/G ratio and mass transfer resistance due to the turbulence and better mixing effect. In the tests of DP-3 (Figure 7D) packing, there also shows consistent mass transfer behavior at different L/G ratios. This is reasonable considering the design of DP-3 packing is very close to that of DP-1 packing. On the other hand, DP-2 (Figure 7C) packing shows an obvious reduction in  $\text{CO}_2$  capture rate at 3.5 L/G since the higher percentage of hydrophobic HIPS segment on the packing surface could reduce the effective reactive film area.

The results prove that our approach to intensify mass transfer through appropriate packing design has been successfully

**FIGURE 6** The  $\text{CO}_2$  absorption efficiency (A) and energy demand (B) at 2.6 L/G ratio and  $\sim 120$  kPa stripping pressure

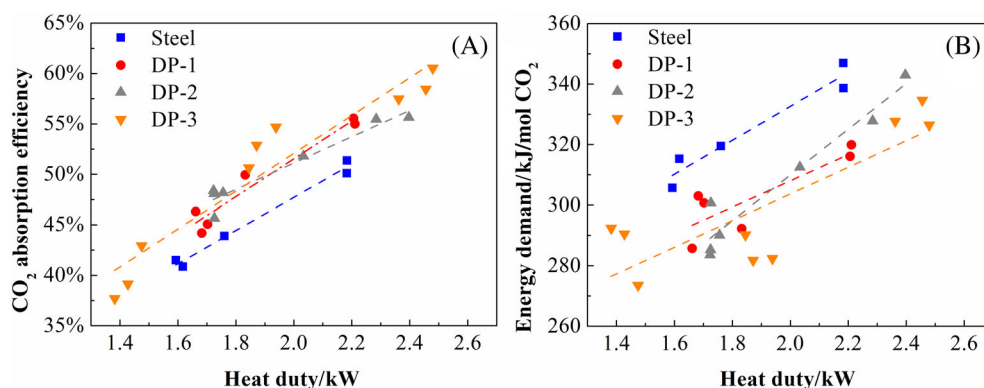
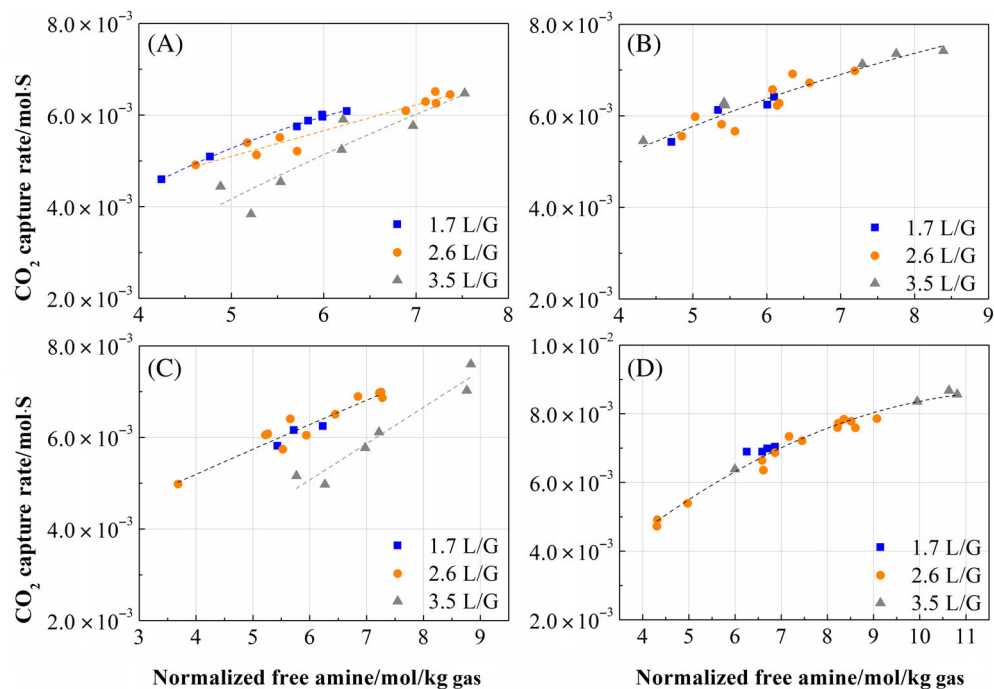


**FIGURE 7** Relationship between  $\text{CO}_2$  capture rate and normalized free amine in lean solvent at different L/G (kg/kg). (A) Mellapak 250Y steel packing; (B) DP-1 packing; (C) DP-2 packing; (D) DP-3 packing (fitting lines are used to guide the eye)



implemented through DP packings. The proper design of DP packing to create local turbulence and refresh liquid film surface can not only eliminate the increase of diffusion resistance resulting from the increased L/G and CO<sub>2</sub> loading but also show the intensified mass transfer for CO<sub>2</sub> absorption in comparison with conventional structured packings. It is expected that the DP-1 and DP-3 packings will show even better performance when they are specifically used to boost solvent CO<sub>2</sub> loading toward a higher loading range based on the previous results. In the best strategy to use DP-3 packings under optimal conditions of 2.6 L/G ratio and 180 kPa stripper pressure, the integrated unit can achieve a steady CO<sub>2</sub> capture with 61.5% efficiency and 277 kJ/mol CO<sub>2</sub> energy demand. This is a relative 22.8% mass transfer improvement in the absorption side and 20.2% energy consumption decrease in the desorption side in comparison with Mellapak 250Y steel packing baseline case under 2.6 L/G ratio and 120 kPa stripper pressure. It is demonstrated that due to the improved mass transfer in the absorber column, the integrated unit achieves a higher CO<sub>2</sub> absorption efficiency and consequential less energy penalty. For the practical operation in a target-based (e.g., 90% CO<sub>2</sub> capture) CO<sub>2</sub> capture, the application of DP packing to intensify mass transfer could benefit the capture process by following the below steps:

1. Reduce the absorber size for low capital cost.
2. Increase the cyclic capacity and decrease the solvent requirement to reduce the solvent cost and pump work.
3. The solvent can be operated at a higher CO<sub>2</sub> loading region and with less water content to reduce energy cost in regeneration.

## 5 | CONCLUSIONS

Three dynamic polarity packings DP-1, DP-2, and DP-3 were developed with the help of 3D printing, which has a hydrophobic shell and the packing surface includes dynamic hydrophilic–hydrophobic segment. The wettability tests verified that nylon and HIPS materials provided ~13 to 18° difference in contact angle at 22°C. The DP packings were tested in a bench-scale integrated CO<sub>2</sub> capture system using Mellapak 250Y steel packing as a baseline. The normalized free amine was proposed to help analyze packing performance in the absorber. Results implied that the DP packings could reduce the diffusion resistance by enhancing turbulence and frequently refreshing the liquid film surface. Therefore, DP packings outperformed conventional steel packings in CO<sub>2</sub> absorption. Combining the employment of DP-3 packings and optimization of operating conditions through parametric study, the integrated unit achieved a steady CO<sub>2</sub> capture with relatively 22.7% increase in absorption efficiency and 20.0% decrease in energy penalty. As only the top three packing elements are replaced by the DP packings, the improvement of unit performance will be even greater if the whole absorber column is equipped with more efficient packings. This will be the goal of our future work in combination with a long-term test regarding the packing stability and its influence on solvent degradation. In addition, this type of packings could potentially speed up CO<sub>2</sub> release from the solvent in stripper through better contact with steam and similar

turbulence effect. The concern would be whether those packing materials can endure high stripping temperature and show both chemical and mechanical stability over a long period.

## ACKNOWLEDGMENTS

The authors acknowledge the U.S. Department of Energy National Energy Technology Laboratory (U.S. DOE, NETL) for the financial support of this project (DE-FE0031661).

## AUTHOR CONTRIBUTIONS

**Min Xiao:** Data curation (lead); formal analysis (equal); investigation (equal); methodology (equal); writing – original draft (lead). **Moushumi Sarma:** Investigation (supporting); validation (equal); writing – review and editing (supporting). **Jesse Thompson:** Conceptualization (equal); data curation (equal); funding acquisition (equal); methodology (equal); project administration (equal) resources (equal) supervision (equal); writing – review and editing (equal). **Du Nguyen:** Conceptualization (equal); resources (equal). **Samantha Ruelas:** methodology (equal); resources (equal). **Kunlei Liu:** Conceptualization (equal); formal analysis (equal); funding acquisition (equal); project administration (equal); supervision (equal); writing – review and editing (equal).

## DATA AVAILABILITY STATEMENT

The data that support the findings of this study are available from the corresponding author upon reasonable request.

## ORCID

Min Xiao  <https://orcid.org/0000-0003-2528-5586>

## REFERENCES

1. Gao W, Liang S, Wang R, et al. Industrial carbon dioxide capture and utilization: state of the art and future challenges. *Chem Soc Rev*. 2020; 49(23):8584–8686.
2. Bui M, Adjiman CS, Bardow A, et al. Carbon capture and storage (CCS): the way forward. *Energ Environ Sci*. 2018;11(5):1062–1176.
3. Tsai RE, Seibert AF, Eldridge RB, Rochelle GT. A dimensionless model for predicting the mass-transfer area of structured packing. *AIChE J*. 2011;57(5):1173–1184.
4. Tan LS, Shariff AM, Lau KK, Bustam MA. Factors affecting CO<sub>2</sub> absorption efficiency in packed column: a review. *J Ind Eng Chem*. 2012;18(6):1874–1883.
5. Gao H, Liu S, Luo X, Zhang H, Liang Z. Investigation of hydrodynamic performance and effective mass transfer area for Sulzer DX structured packing. *AIChE J*. 2018;64(10):3625–3637.
6. Xu B, Gao H, Luo X, Liao H, Liang Z. Mass transfer performance of CO<sub>2</sub> absorption into aqueous DEEA in packed columns. *Int J Greenh Gas Control*. 2016;51:11–17.
7. Aroonwilas A, Veawab A, Tontiwachwuthikul P. Behavior of the mass-transfer coefficient of structured packings in CO<sub>2</sub> absorbers with chemical reactions. *Ind Eng Chem Res*. 1999;38(5):2044–2050.
8. Tsai RE, Schultheiss P, Kettner A, et al. Influence of surface tension on effective packing area. *Ind Eng Chem Res*. 2008;47(4):1253–1260.
9. Moore T, Nguyen D, Iyer J, Roy P, Stolaroff JK. Advanced absorber heat integration via heat exchange packings. *AIChE J*. 2021;67(8):e17243.



10. Frimpong RA, Nikolic H, Bahr D, Kiran G, Liu K. Pilot scale testing of an advanced solvent in a 0.7 MWe post-combustion CO<sub>2</sub> capture unit. *Int J Greenh Gas Control*. 2021;106:103290.
11. Baltar A, Gómez-Díaz D, Navaza JM, Rumbo A. Absorption and regeneration studies of chemical solvents based on dimethylethanolamine and diethylethanolamine for carbon dioxide capture. *AIChE J*. 2020;66(1):e16770.
12. Song D, Seibert AF, Rochelle GT. Effect of liquid viscosity on mass transfer area and liquid film mass transfer coefficient for GT-OPTIMPAK 250Y. *Energy Procedia*. 2017;114:2713-2727.
13. Suess P, Spiegel L. Hold-up of mellapak structured packings. *Chem Eng Process*. 1992;31(2):119-124.
14. Janzen A, Steube J, Aferka S, et al. Investigation of liquid flow morphology inside a structured packing using X-ray tomography. *Chem Eng Sci*. 2013;102:451-460.
15. Nicolaiewsky EMA, Tavares FW, Rajagopal K, Fair JR. Liquid film flow and area generation in structured packed columns. *Powder Technol*. 1999;104(1):84-94.
16. Bradtmöller C, Janzen A, Crine M, Toye D, Kenig E, Scholl S. Influence of viscosity on liquid flow inside structured packings. *Ind Eng Chem Res*. 2015;54(10):2803-2815.
17. Moganty SS, Baltus RE. Diffusivity of carbon dioxide in room-temperature ionic liquids. *Ind Eng Chem Res*. 2010;49(19):9370-9376.
18. Hu J, Liu J, Yu J, Dai G. CO<sub>2</sub> absorption into highly concentrated DEA solution flowing over a vertical plate with rectangular windows. *Int J Greenh Gas Control*. 2013;19:13-18.
19. Kohrt M, Ausner I, Wozny G, Repke J-U. Texture influence on liquid-side mass transfer. *Chem Eng Res Des*. 2011;89(8):1405-1413.
20. Sun B, Zhu M, Liu BT, Liu CJ, Yuan XG. Investigation of falling liquid film flow on novel structured packing. *Ind Eng Chem Res*. 2013;52(13):4950-4956.
21. Sarma M, Abad K, Bhatnagar S, et al. Matching CO<sub>2</sub> capture solvents with 3D-printed polymeric packing to enhance absorber performance. Paper presented at: Proceedings of the 15th Greenhouse Gas Control Technologies Conference; March 15–18, 2021; Abu Dhabi.
22. Jayarathna SA, Weerasooriya A, Dayarathna S, Eimer DA, Melaaen MC. Densities and surface tensions of CO<sub>2</sub> loaded aqueous monoethanolamine solutions with  $r = (0.2 \text{ to } 0.7)$  at  $T = (303.15 \text{ to } 333.15)$  K. *J Chem Eng Data*. 2013;58(4):986-992.
23. García-Abuín A, Gómez-Díaz D, Navaza JM, Sanjurjo B. Effect of surfactant nature upon absorption in a bubble column. *Chem Eng Sci*. 2010;65(15):4484-4490.
24. Gómez-Díaz D, Navaza JM, Sanjurjo B. Mass-transfer enhancement or reduction by surfactant presence at a gas–liquid interface. *Ind Eng Chem Res*. 2009;48(5):2671-2677.
25. Hebrard G, Zeng J, Loubiere K. Effect of surfactants on liquid side mass transfer coefficients: a new insight. *Chem Eng J*. 2009;148(1):132-138.
26. Li K, Cousins A, Yu H, et al. Systematic study of aqueous monoethanolamine-based CO<sub>2</sub> capture process: model development and process improvement. *Energy Sci Eng*. 2016;4(1):23-39.
27. Xiao M, Zheng W, Liu H, Tontiwachwuthikul P, Liang Z. Analysis of equilibrium CO<sub>2</sub> solubility and thermodynamic models for aqueous 1-(2-hydroxyethyl)-piperidine solution. *AIChE J*. 2019;65(6):e16605.

## SUPPORTING INFORMATION

Additional supporting information may be found in the online version of the article at the publisher's website.

**How to cite this article:** Xiao M, Sarma M, Thompson J, Nguyen D, Ruelas S, Liu K. CO<sub>2</sub> absorption intensification using three-dimensional printed dynamic polarity packing in a bench-scale integrated CO<sub>2</sub> capture system. *AIChE J*. 2022; 68(4):e17570. doi:10.1002/aic.17570